

ULTRASONIC FIELD COMPUTATION INTO MULTILAYERED COMPOSITE MATERIALS USING A HOMOGENIZATION METHOD BASED ON RAY THEORY

S. Deydier¹, N. Gengembre¹, P. Calmon¹, V. Mengeling², O. Pétillon²

¹ Commissariat à l'énergie Atomique, LIST, CEA-Saclay, bât. 611, 91191 Gif-sur-Yvette cedex, France

² EADS/CCR, BP 76, 12 rue Pasteur, 92152 Suresnes cedex, France

ABSTRACT. The simulation of ultrasonic NDT of carbon-fiber-reinforced epoxy composites (CFRP) is an important challenge for the aircraft industry. In a previous article, we proposed to evaluate the field radiated into such components by means of a homogenization method coupled to the pencil model implemented in CIVA software. Following the same goals, an improvement is proposed here through the development of an original homogenization procedure based on ray theory.

INTRODUCTION

The aircraft industry shows a growing interest for the simulation of ultrasonic non destructive testing, which gives powerful tools for analyzing experimental results and optimizing testing configurations. This paper deals with a study dedicated to the modeling of ultrasonic propagation in carbon-fiber-reinforced epoxy composites (CFRP), whose engineered shapes are getting more and more complex.

The studied multilayers can be made of periodical stacking sequences of a carbon-epoxy pattern (for instance a [(00/+45/-45/90)] pattern as in Fig. 1), the typical size of one layer being 100-300 μm . The unidirectional layers forming a pattern may also present different ratios and, due to the complex shapes, may not be parallel all together [1] (see Fig. 2). A realistic simulation must take into account both the effects of the material and those due to the complex geometry of the component. To fulfill these requirements, one has worked with the field computation capabilities of the software platform CIVA. This module is based upon the so-called pencil method, and dedicated to the computation of transmitted ultrasonic beams emitted by transducers into anisotropic or/and heterogeneous materials [2].

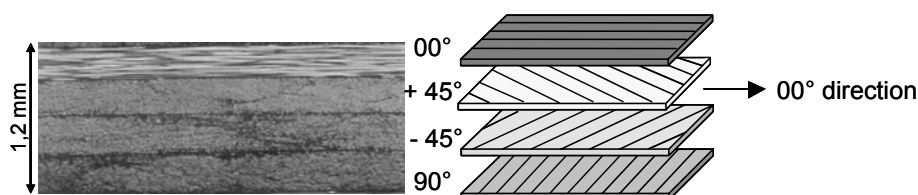


FIGURE 1. Micrograph of a 1,2-mm-thick pattern containing four unidirectional layers.

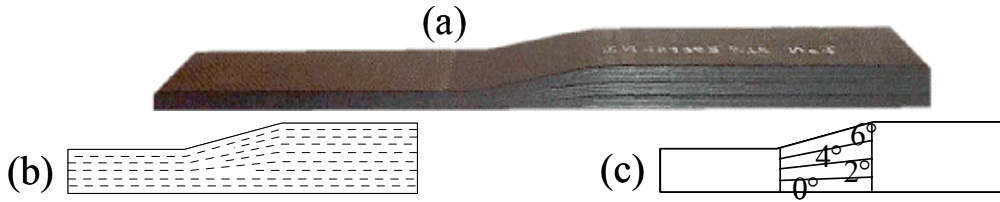


FIGURE 2. a- Carbon-epoxy piece with parallel and non-parallel layers (slope: 8°). b- Schematic view of the layers. c- Same component after homogenization: parallel parts are simplified with one homogeneous material whereas non-parallel ones are replaced by the same homogeneous materials whose symmetry axis is progressively rotated (0° , 2° , 4° and 6°).

The approach adopted here consists in coupling this model with a homogenization method allowing to describe the layered structure into one homogeneous anisotropic effective medium for parallel layers, and into a heterogeneous medium made of several volumes (see Fig. 2-c) when the geometry of the component implies that layers are not exactly parallel.

This work follows a previous study [1] in which a homogenization based on Postma's method had been applied, assuming static deformations (i.e. low frequency approximation). The analysis of the first results proved the interest of the approach but led us to work on improving the homogenization procedure itself. Our work is also based on a model that predicts the effective stiffness constants and attenuation (fiber multiple scattering coupled with epoxy viscoelastic losses) of a single layer.

In the first part of this paper, we present a new homogenization method, based on ray theory, and called in the following Ray theory Based Homogenization (RBH). An example of a multilayer material simplified by this means is presented. In a second part, the capabilities of the method are demonstrated through field computations using different homogenization methods and computations with the whole layers. In the third part, comparisons with experiments are discussed.

RAY THEORY BASED HOMOGENIZATION

Introduction

The Ray theory Based Homogenization (RBH) proposed here aims at obtaining the effective stiffness constants by synthesizing an effective slowness surface deduced from ray tracing modeling. This procedure is achieved considering the periodicity of the composites as described previously, i.e. only one pattern (period) of the component needs to be considered. The method can also be used when the pattern contains layers with different thicknesses, which allows to homogenize materials containing layers in unequal proportions

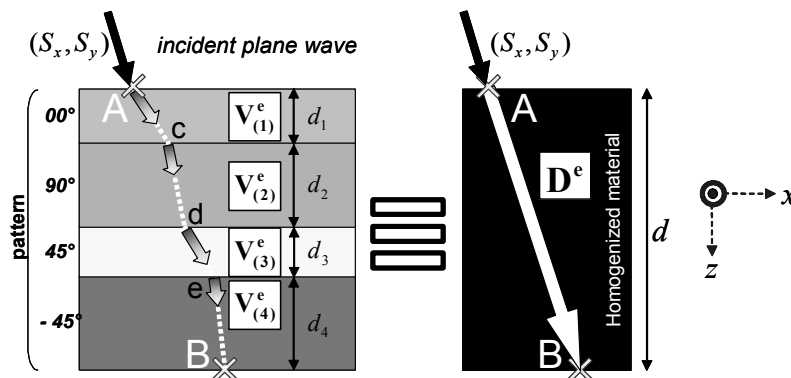


FIGURE 3. Ray theory Based Homogenization: the follow-up of the energy path in one pattern (left) leads to an average energy direction $\overline{AB}=\mathbf{D}^e$ supposed to be that in the homogenized equivalent material (right).

(the representative pattern is then defined using the layer ratios as thicknesses). This is possible since the method does not depend on the order of the layers.

The RBH method is carried out by following the energy ray path inside each ply of the pattern under consideration, which gives access to an average energy direction (as shown in Fig. 3). The relationship between phase and energy directions leads to the geometrical construction of an overall slowness surface describing an anisotropic homogeneous medium, characterizing the whole composite. An optimization method is then applied to obtain the associated effective stiffness tensor, which is then used in the simulations. These steps are described below.

Energy Ray Path

Let us consider an incident plane wave, represented by its slowness components along x- and y-axes (parallel to the interfaces), say S_x and S_y . The energy ray path is entering inside the studied pattern at point **A** and propagates toward an exit point **B**, defined in Fig. 3. The vector **AB** is supposed to be an average energy ray direction $\mathbf{D}^e = \mathbf{AB}$ in the homogenized material and is written as:

$$\mathbf{AB} = \mathbf{Ac} + \mathbf{cd} + \mathbf{de} + \mathbf{eB} = \sum_{m=1}^4 t_m \cdot \mathbf{V}_{(m)}^e = \sum_{m=1}^4 \frac{d_m}{V_{(m)z}^e} \cdot \mathbf{V}_{(m)}^e = \mathbf{D}^e, \quad (1)$$

where **c**, **d**, and **e** are intersection points of the ray with the internal surfaces. The amounts t_m , d_m and $\mathbf{V}_{(m)}^e$ are respectively the energy propagation time, thickness and energy speed vector in the m^{th} layer. In order to obtain $\mathbf{V}_{(m)}^e$, the Christoffel's equation [4] is solved in Cartesian coordinates, the only unknown being the z-slowness (S_x and S_y are retained inside every layers, according to Descartes' law). One has:

$$\left| C_{ijkl}^{(m)} \cdot S_j^{(m)} \cdot S_l^{(m)} - \rho \cdot \delta_{ik} \right| = \left| G_{ik}^m \right| = 0, \quad (2)$$

where the $C_{ijkl}^{(m)}$ are the m^{th} layer stiffness constants, ρ the density of the component and G_{ik}^m the Christoffel's matrix. Inside each layer, developing equation (2) leads to a 6th order polynomial, with six solutions among which three at most are suitable (i.e. with down going energy). By calculating the eigenvectors of the Christoffel's matrix, the polarization vector \mathbf{u}^m is obtained and the energy velocity vector writes:

$$G_{ik}^m \cdot u_k^m = 0 \quad \text{then} \quad V_{(m)}^e = \frac{C_{ijkl}^{(m)} \cdot u_j^m \cdot u_l^m \cdot S_k^m}{\rho} \quad (3)$$

Repeating such a process for each layer constituting the pattern leads to the vector \mathbf{D}^e (normalized direction: \mathbf{D}_N^e).

Geometrical Building of the Slowness Surface

For CFRP materials, the layers are constituted of the same material with disorientations around the z-axis. Hence, at normal incidence, $(S_x, S_y) = (0, 0)$ and the z-slowness has the same value inside each layer, easily calculable using Christoffel's equation. Thus, the very first point of the slowness surface $\mathbf{P}^{(0)}$ is exactly known. For the 3D reconstruction of the slowness surface, one considers successive planes rotating around z-axis and defined by base vector \mathbf{e}_φ .

In each plane (\mathbf{e}_φ, z) , successive points $\mathbf{P}^{(i)}$ of the slowness surface are computed in an iterative way by applying the relationship between phase and energy directions: the normal to the effective slowness curve at any abscissa (S_x, S_y) is the averaged energy

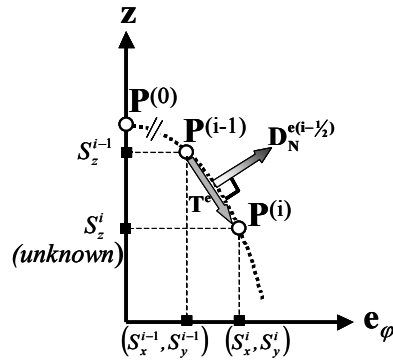


FIGURE 4. Ray theory Based Homogenization: iterative building of a synthesized slowness surface, using the relationship between phase and energy directions.

direction \mathbf{D}^e evaluated with the method described above. The normal to \mathbf{D}^e in the plane (\mathbf{e}_φ, z) is the tangent to the curve under construction, say \mathbf{T}^e . If $\mathbf{P}^{(i-1)}$ is known and if \mathbf{T}^e is evaluated at half step $(i-1/2)$, the next point $\mathbf{P}^{(i)}$ can be built (see Fig. 4).

Effective Stiffness Constants

A fast optimization procedure is then used in order to find the effective stiffness constants leading to the best fit of slowness surfaces. Assuming that the homogenized medium symmetry is known (for example transversely isotropic or hexagonal) a function derived from the Christoffel equation (2) is minimized, following [5].

EXAMPLE OF RBH AND COMPARISON WITH POSTMA'S METHOD

RBH Homogenization of [(00/90/+45/-45)] Carbon-Epoxy

Let us consider the example of a [(00/90/+45/-45)] carbon-epoxy composite whose pattern is constituted by layers of equal thickness. The RBH procedure has been applied to this material. The resulting QP slowness curve is shown on Fig. 5 and compared with the QP slowness curve predicted by applying Postma's method. It can be seen that RBH predicts a greater sensitivity to phase direction angle than Postma's method, and a greater deviation between phase and energy directions appears at large incidences.

The set of stiffness constants describing this material is computed by means of the optimization procedure described above, and assuming hexagonal symmetry. Fig. 6 shows both the slowness curves, in xz -plane, built in the first step and the ones recomputed with

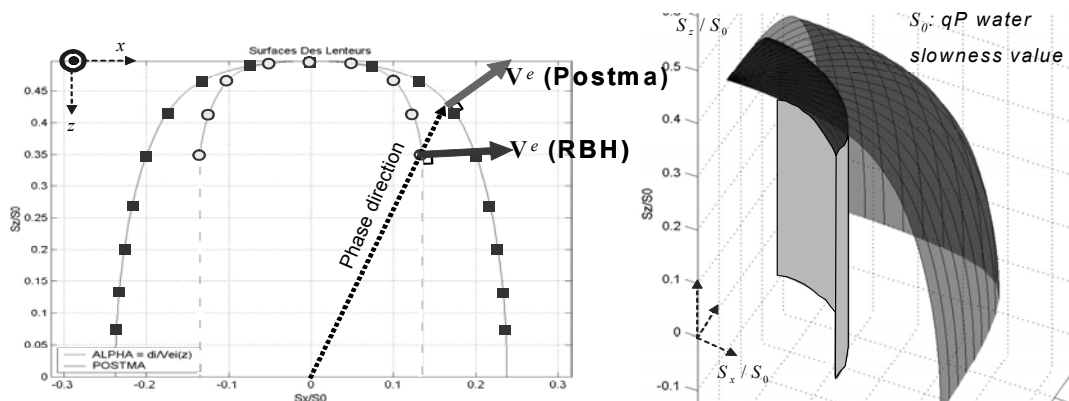


FIGURE 5. Example of QP slowness surfaces: comparison between Postma Homogenization (black squares on left, clear grey on right) and RBH (circles on left, dark grey on right). 2-D (left) and 3-D (right) slownesses show the energy divergence between the two methods, in the same phase direction.

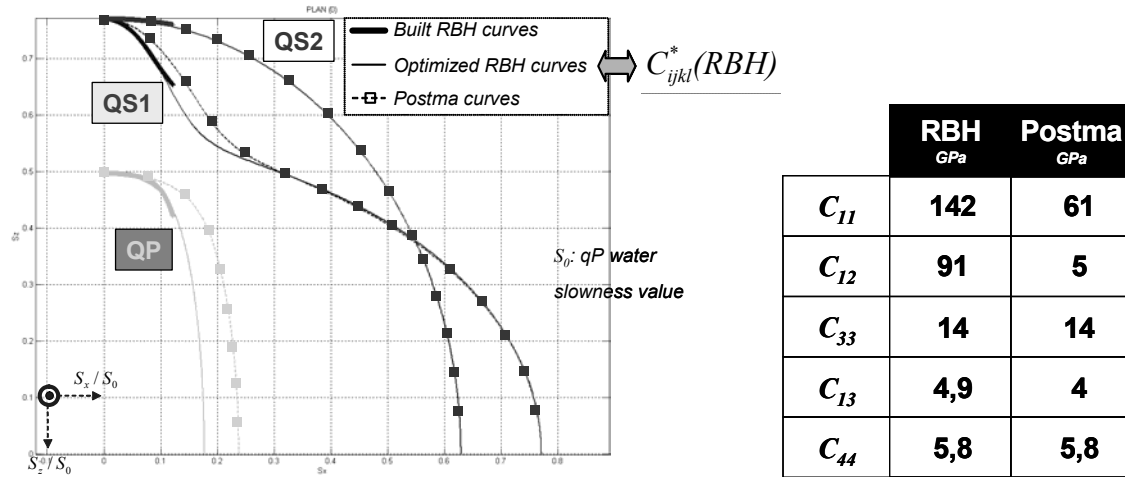


FIGURE 6. Left: slowness surfaces comparison between Postma Homogenization and optimized Ray theory Based Homogenization, for the 3 propagation modes. Right: effective stiffness constants of the 2 methods based on orthotropic assumption of the homogenized component.

the effective stiffness constants. The curves are again compared with the ones obtained with Postma's method, both sets of constants being indicated on the right part of the Fig.6.

The major differences between the two homogenization methods appear for QP modes when the incident angle increases. In this case the wave number decreases more abruptly for RBH method. The influence of these differences on the computed fields in realistic testing configurations is studied in the next section.

Comparison Between Postma's and RBH Methods by Simulation of Transmitted Beams

The final objective of the homogenization method is here the stiffness tensor of the homogenized material as input of transmitted fields computation. Therefore, the relative quality of the two homogenization methods can be evaluated by comparing the corresponding computed beams with the beam obtained without homogenization of the material (every layers being considered). Such comparisons have been performed on QP fields computed in CIVA in the case of a [(00/90/+45/-45)] composite structure constituted of 20 layers, the proportions of each orientation being respectively 50%, 10%, 20% and 20%. In the case of non-homogenized material, only the first arrival contributions are taken into account (the contributions of inner multiple reflections are negligible). In addition, in order to allow quantitative comparisons in the three cases the attenuation is set to zero.

Simulations of fields transmitted in a planar part by immersion transducers of varying frequency and under different incidences have been performed. On Fig. 7 are reported the

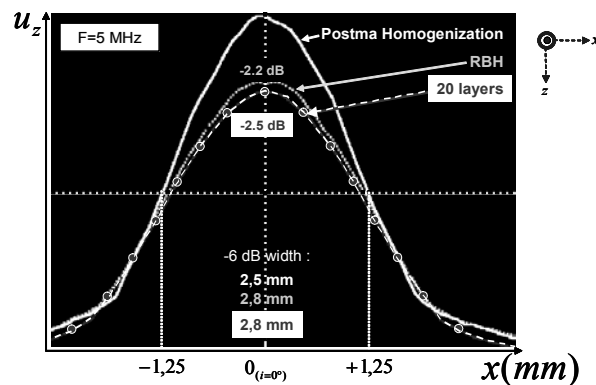


FIGURE 7. QP mode echodynamics computed by CIVA software. RBH and Postma homogenizations are compared to a 20 layers result at normal incidence, 5 MHz transducer frequency.

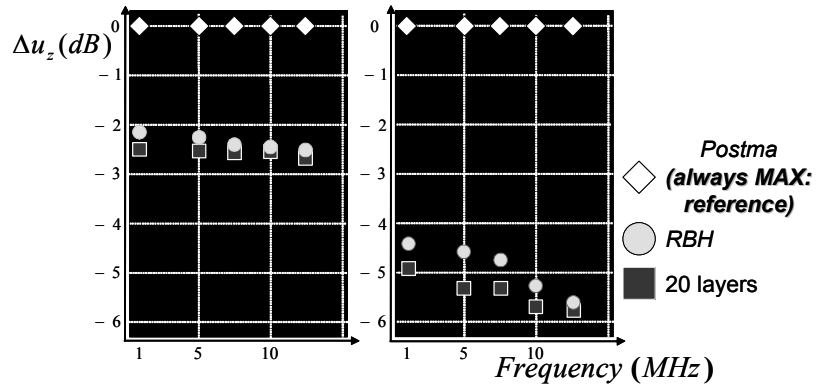


FIGURE 8. Z-displacement fields maxima computed by Champ-Sons. Amplitudes evolution with the transducer frequency (MHz) when the QP incident angle is null (left) or 4° (right).

amplitude distributions of u_z (u_z being the displacement component normal to the surface) through the 20 layers homogenized or not, obtained at 5 MHz, at normal incidence and along x-axis.

Fig. 8 shows the variation of the maximal amplitude of u_z at an incidence of 0° and 4°, versus frequency. It can be seen that RBH predictions are much closer to the results computed by taking into account the multi-layered structure than Postma's homogenization predictions. The discrepancies observed when applying Postma's method increases with frequency and incident angle.

EXPERIMENTAL VALIDATION

A set of experiments have been performed in order to validate the approach on realistic complex situations. The component under study is shown on Fig. 2: its incoming surface presents two horizontal areas with two different thicknesses, separated by a tapered region in which the number of layers increases progressively. An immersion transducer (diameter 12.7mm, frequency 5MHz) is used at vertical incidence. Four different positions

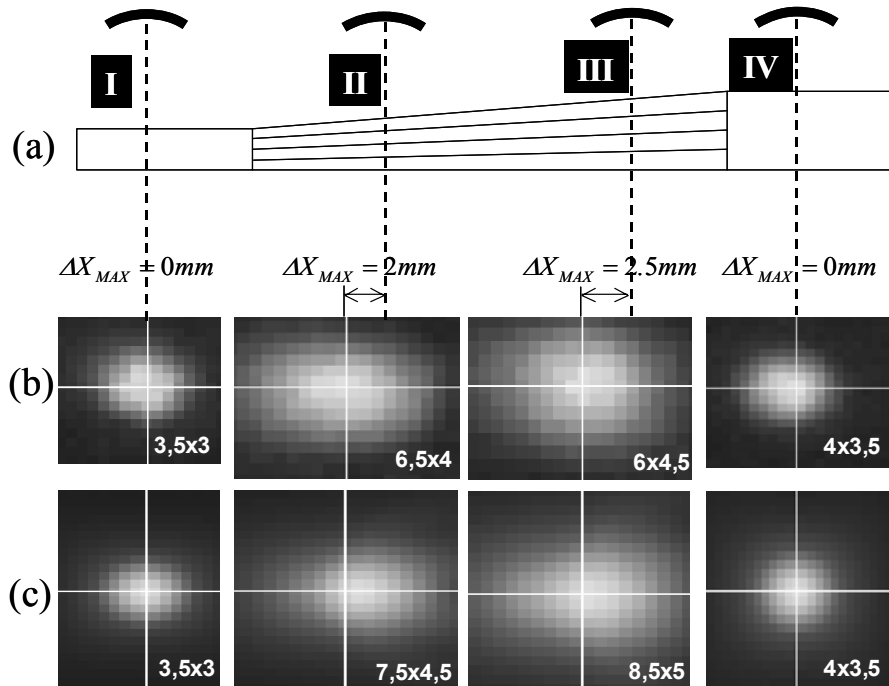


FIGURE 9. a- Definition of the four positions of the transducer. b- Transmitted fields (vertical particle displacements) measured for the different positions, beam width and height in mm being indicated. c- Simulated fields using RBH.

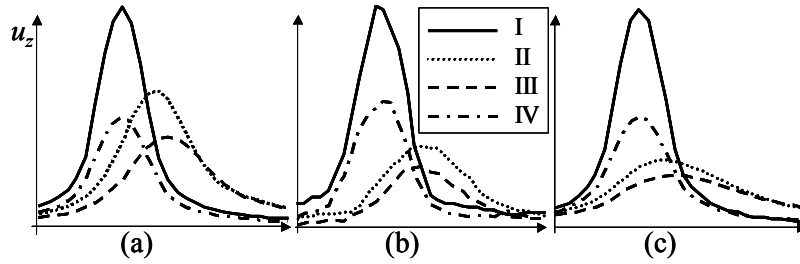


FIGURE 10. Transmitted fields along x-axis (a- Postma's approach, b- experiment, and c-RBH approach). The four positions of the transducer are superimposed, in a coordinate system relative to the transducer.

I, II, III and IV have been defined (see Fig. 9-a) for the transducer in order to cover the various situations occurring during the real inspection of such a geometry. Positions I and IV, on the horizontal parts, correspond to normal incidence (horizontal surface) whereas positions II and III, over the slope, correspond to an 8° incident angle. For each position, the field transmitted through the piece is measured by scanning a receiver positioned at the back wall surface. This receiver is small enough so that its diffraction is negligible, and the received signal evolution can be directly compared to calculations of the vertical component of the displacement field.

Fig. 9-b shows the transmitted fields measured in the four configurations, which are compared to the computed field using homogenized media with RBH method in Fig. 9-c. These simulations have been performed by considering that the material under the slope can be defined by a small number of areas constituted of the same homogenized anisotropic material but with disoriented axes, as in Fig. 2. The horizontal deflection of the beam, say ΔX_{MAX} (i.e. the distance between the axis of the transducer and the center of the outgoing beam) is correctly predicted. The good agreement between computations and experiments validates the latter assumption, as it validates the homogenization approach.

Once again, comparisons with Postma's method have been done. Fig. 10 shows a comparison between experimental measurements and computation results with RBH and Postma. The transmitted field at the back wall surface is computed or measured along x-axis for every transducer positions, the x-coordinate in the graph being evaluated relatively to the transducer x-position, which allows to superimpose the different results. Again, the beam deviations for positions II and III are observed and predicted by both homogenization methods. In Fig. 10, the similar shape of the three graphs permits to validate the approach consisting in replacing the whole layers with a homogenized material. The improvements made by the RBH method are also emphasized: the absolute amplitudes predicted using this homogenization are closer to the fields measured than the ones predicted using Postma's method. In order to underline this, the maximum amplitude of each curve has been reported on the graph of Fig. 11. This amount is plotted as a function of the position of the transducer and for each configuration (measured, Postma and RBH). Since one aims here at

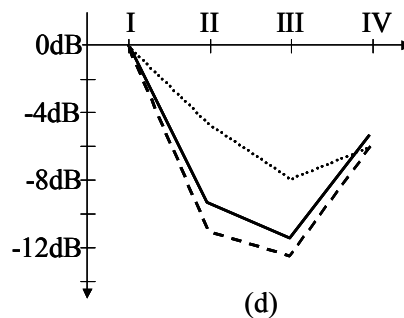


FIGURE 11. Evolution of the maximum amplitudes for the field transmitted through the component at the 4 positions described on Fig. 9. Solid line = experiment, dashed line = computation with RBH homogenization, dotted line = computation with Postma's homogenization.

comparing the relative evolution of the maximum amplitudes, the three curves have been normalized with respect to their value at position I. It can be seen that a better agreement is found between RBH and experiment than between Postma and experiment.

CONCLUSION

In this paper we present a modeling approach based on homogenization for predicting ultrasonic fields propagating in multilayered CFRP. A homogenization method based on ray theory is proposed. The advantages of this method relatively to the more classical Postma's method are estimated both theoretically and experimentally. At last the reliability of ultrasonic fields predictions in complex situations is shown by comparing computations results and experimental measurements.

REFERENCES

1. Gengembre, N., Calmon, P., Petillon, O. and Chatillon, S., in *Review of Progress in QNDE*, Vol. 22, eds D. O. Thompson and D. E. Chimenti, AIP Conference Proceedings, Melville, 2003, p. 957.
2. Gengembre N. and Lhémery A., *Review of Progress in QNDE*, Vol. 19, *op. cit.* (2000), p. 977.
3. Lonné, S., Lhémery, A., Calmon, P., Biwa, S. and Thévenot, F., *Review of Progress in QNDE*, Vol. 23, *op. cit.* (2004), p. 875.
4. Royer, D. and Dieulesaint, E., *Ondes élastiques dans les solides*, Tome 1, Masson, 1996.
5. Aristégui, C. and Baste, S., *J. Acoust. Soc. Am.*, **102**, 1503 (1997).
6. He, P. and Zheng, J., *Ultrasonics*, **39**, 27 (2001).

KEYWORDS

1. Anisotropic multilayers
2. Homogenization
3. UT simulation
4. Ray theory